2011 American Control Conference
on O'Farrell Street, San Francisco, CA, USA
June 29 - July 01, 2011

# Optimal Input Design for Indentation-based Rapid Broadband Nanomechanical Spectroscopy: Poly(dimethylsiloxane) example†

Zhonghua Xu, Qingze Zou ‡

*Abstract*— **This article presents an optimal input design approach to achieve rapid broadband nanomechanical measurements of soft materials using the indentation-based method. The indentation-based nanomechanical measurement provides unique quantifications of material properties at specified locations. The measurements, however, are currently too slow in time and too narrow in frequency (range) to characterize time-elapsing material properties during dynamic evolutions (e.g., the rapid-stage of the crystallization process of polymers). Such limits exist because the input force profiles used in current approaches cannot rapidly excite broadband nanomechanical properties of materials. In this article, we develop an optimal-input design approach to tackle these challenges. Particularly, an input force profile with discrete spectrum is optimized to maximize the Fisher information matrix of the linear compliance model of the soft material. Both simulation and experimental results on a PDMS sample are presented to illustrate the need for optimal input design, and its efficacy in probe-based nanomechanical property measurements.**

## I. Introduction

In this article, an optimal input design approach is proposed to achieve rapid identification of broadband nanomechanical properties of soft materials using indentation-based approach. Indentation-based approach using scanning probe microscope (SPM) or nanoindentator has become an enabling tool to quantitatively measure the nanomechanical properties of a wide variety of materials both locally and globally [1]. The current measurement methods [2], [3], however, are limited in both the frequency range that can be measured and the time duration that is needed to measure the (frequency) rate-dependent viscoelasticity of materials. Such limits of current measurement methods [2], [3], in both measurement frequency and time, arise as the excitation input (i.e., the force applied from the probe to the sample surface) used cannot: (1) compensate for the convolution effect of the instrument dynamics when the measurement frequency becomes high [4] and (2) rapidly excite the rate-dependent nanomechanical behavior of the material when the material properties are changing during the measurements. These inabilities of the excitation force profile used in current nanomechanical measurements, thereby, motivate the work presented in this paper to meet the challenges in emerging nanomechanics studies.

Inefficiencies exist in current nanomechanical measurement methods for characterizing the time-elapsing material properties. The excitation force used in conventional force-curve measurements [1] is quasi-static and thereby, does not contain rich frequency components required to rapidly excite viscoelastic response of materials. The lack of frequency components in the excitation force can be alleviated by using the force modulation technique [2]. The instrument dynamics effect, however, can be coupled into the measured data, and the force-modulation is slow to sweep a large frequency range. The measurement time can be reduced by using the recently-developed multi-frequency method [3], however, the frequency components selected are not optimized, and the measurement frequency range is still limited by the instrument dynamics coupling effect. Evidently, there is a need to improve the current indentation-based nanomechanical property measurement approaches.

One main challenge to achieve rapid broadband nanomechanical measurement is to ensure that (1) the force applied shall accurately track the desired force and (2) the indentation should be accurately measured. Tracking of the desired force profile is necessary to (1) excite the material behavior in the measured frequency range, and (2) avoid issues related to low signal-to-noise ratio and input saturation (due to the force being too small or too large), while the indentation measured should capture the material behavior well—as the response to the force applied. When the measurement frequency range becomes large (i.e., broadband), however, the dynamics of the system consisting of the piezo actuator and the probe can be excited along with the nonlinear hysteresis effect of the piezo-actuators, resulting in large vibrations of the probe relative to the sample. Furthermore, substantial dynamics uncertainties exist in the SPM system due to the thermal drift and the change of operation condition (e.g., change of the probe). These adverse effects can be mitigated by using control techniques, as demonstrated recently by using the iterative learning control methods [4], [5]. Residual instrument dynamics effect, however, still exists in the indentation measured. Recently, model-based techniques [4] have been developed to account for the dynamics convolution effect on the measured indentation data. These post-processing technique, however, cannot be used to achieve rapid broadband nanomechanical measurements, as discussed next.

The other major challenge in rapid broadband nanomechanical measurements is to achieve rapid excitation of the material response in the measured frequency range by the force applied (from the probe). Rapid excitation (of the material response) is needed to capture the time-elapsing nanomechanical properties during the dynamic evolution of the material, as well as to map the nanomechanical

† The financial support of NSF CAREER award CMMI-0846350 is gratefully acknowledged.

‡ Z. Xu is with Mechanical Engineering, Iowa State University, Ames, IA, USA 50011. Q. Zou is with Mechanical and Aerospace Engineering, Rutgers University, NJ, USA. Q. Zou is the corresponding author (qzzou@rci.rutgers.edu).

properties of the material over the sample surface. Recently a frequency-rich excitation force with power spectrum similar to band-limited white noise has been utilized for broadband nanomechanical measurement [5]. Although the iterative learning control (ILC) technique has been applied for the tracking of such a complicated desired trajectory, dynamics convolution effect discussed above still exists. Thus, these two major challenges in rapid broadband nanomechanical measurements are both closely related to the excitation force applied (from the probe to the sample surface).

The main contribution of this article is the development of an approach based on the optimal input design to address the above two challenges in achieving rapid nanomechanical spectroscopy. First, the measurement of nanomechanical properties is transformed into a parameter identification problem by combining the tip-sample contact model with the mechanics model of the soft material [6]. Then, an optimal excitation force is sought to minimize the covariance of the estimation error through the maximization of the Fisher information matrix [7], [8] of the parameterized mechanics model. The designed optimal excitation force profile (e.g., the cantilever deflection when using SPM) is tracked by using the recently-developed inversion-based iterative control technique that compensates for the hardware dynamics convolution effect. The proposed approach is illustrated through both simulation and experimental implementation on the measurement of viscoelasticity of a Polydimethylsiloxane (PDMS) sample using a scanning probe microscope. The simulation and experiment results demonstrate the need of optimal input design and the efficacy of the proposed approach in achieving broadband viscoelasticity spectroscopy.

## II. Optimal Input Design for Rapid Nanomechanical Spectroscopy

We start by transforming the nanomechanical property measurement into a parameter estimation problem.

### A. Parameter Estimation in Nanomechanical Measurement

SPM has become a powerful tool to characterize various material properties at nanoscale (e.g., [9]), through the measurement of the tip-sample interaction force and the tip indentation on the sample surface, i.e., the force curve measurement, which is obtained by measuring the tip-sample interaction force and the vertical displacement of the SPM-tip during the process when a micro-fabricated cantilever with a nanometer-radius tip is driven by a piezoelectric actuator to push against and then retrace from the sample surface (see Fig. 1(a)). The indentation is obtained from the difference between the cantilever deflection on the soft sample and that on a reference hard sample when the same control input voltage is applied to the piezo actuator during the force curve measurement of the reference hard material. Such an indentation-based approach allows the material properties to be quantitatively measured at desired locations with desired force amplitude with nanoscale spatial resolutions.

To identify material properties, the measured force and indentation results are utilized as the input and output data in an appropriate mechanics model to identify nanomechanical

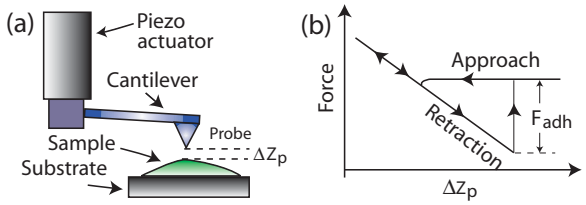

Fig. 1. The scheme of force curve measurement by SPM

properties of materials [1]. For example, when the Hertz contact mechanics model is employed, the creep compliance of the material, $J(\cdot)$, can be quantified by using the measured tip-sample interaction force, $P(\cdot)$, and the indentation in the material, $h(\cdot)$, by

$$h^{\frac{3}{2}}(t) = \frac{9}{16\sqrt{R}} \int_0^t J(t-\tau) \frac{dP(\tau)}{d\tau} d\tau, \tag{1}$$

where $R$ is the tip radius. The Hertz contact mechanics model captures the frequency dependent nanomechanical property of the material [6]. To further characterize the nanomechanical properties and different response speed of materials to the excitation force, the parameterized model of the material complex compliance $J(\cdot)$ has been proposed [6]. In this article, we use a truncated Prony series to model the creep compliance,

$$J(t) = J_0 - \sum_{i=1}^{n} J_i \cdot e^{-t/\tau_i}, \tag{2}$$

where $J_0$ is the fully relaxed compliance, $J_i$s are the compliance coefficients, and $\tau_i$s are the discrete retardation times.

Combining Eq. (1) with (2) implies that the creep compliance $J(t)$ can be viewed as a linear time-invariant mapping between the force $P(t)$ and the effective indentation, $h(t)$,

$$J(t) : u(t) \triangleq \frac{9P(t)}{16\sqrt{R}} \longrightarrow h^{\frac{3}{2}}(t) \triangleq y(t), \tag{3}$$

which can be converted into the following autoregressive exogenous model (ARX) [10]

$$y(\ell) + \sum_{i=1}^{n_a} a_i y(\ell - i) = \sum_{i=1}^{n_b} b_i u(\ell - i), \tag{4}$$

where $n_a$ is the number of poles, $n_b$ is the number of zeros plus 1, $\ell$ is the $\ell^{th}$ sampling instance, and the unknown parameters $a_i$s and $b_i$s are related to the original retardation time constants $\tau_i$s and compliance coefficients $J_i$s through

$$J_0 = k - \sum_{i=1}^{n} \frac{r_i}{p_i}; \quad J_i = \frac{r_i}{p_i}; \quad \tau_i = -\frac{1}{p_i}. \tag{5}$$

As in the standard parameter identification [10], the above discrete model (4) is then rewritten as an affine function of the unknown parameters $\theta$, $y(\ell) = \varphi^T(\ell)\theta$, with $\theta$ the vector of unknown parameters $\theta = [a_1, \ldots, a_{n_a}, b_1, \ldots, b_{n_b}]^T$, and $\varphi(\ell)$ the sequence of measured input and output data, i.e., $\varphi(\ell) = [-y(\ell-1), \ldots, -y(\ell-n_a), u(\ell-1), \ldots, u(\ell-n_b)]^T$.

Thus, the least-square estimation of the linear compliance model parameter, $\widehat{\theta}_N$, can be obtained by

$$\begin{aligned} \min_{\theta} V_N(\theta, Z^N) &= \min_{\theta} \frac{1}{N} \sum_{\ell=1}^{N} [y(\ell) - \widehat{y}(\ell|\theta)]^2 \\ &= \min_{\theta} \frac{1}{N} \sum_{\ell=1}^{N} [y(\ell) - \varphi^T(\ell)\theta]^2, \end{aligned} \tag{6}$$

where $Z^N$ denotes the set of past inputs and outputs over the time interval $1 \le \ell \le N$, and $\widehat{y}(\ell|\theta)$ denotes the output computed by the estimated parameters $\theta$, $\widehat{y}(\ell|\theta) = \varphi^T(\ell)\theta$. The obtained optimal parameter estimation is given by

$$\widehat{\theta}_N = \left[\sum_{\ell=1}^{N} \varphi(\ell)\varphi^T(\ell)\right]^{-1} \sum_{\ell=1}^{N} \varphi(\ell) y(\ell), \tag{7}$$

After the discrete *ARX* model is identified, the unknown parameters in the linear compliance model (2) can be obtained from the mapping (5) after discrete-to-continuous conversion and partial fraction expansion.

To utilize the above parameter estimation approach in nanomechanical measurements, the input force needs to be carefully designed. Note that the applied force is generated by the driven voltage sent to the piezoactuator (see Fig. 1(a)), the convolution of the input with the dynamics from the piezo actuator to the cantilever can thereby, lead to distortions in the excitation force. As a result, the distorted force may fail to excite the nanomechanical properties of interests. Therefore, optimal input design is proposed to avoid the instrument dynamics effect, and achieve rapid and accurate parameter estimations in nanomechanical measurements.

### *B. Optimal Input Design for Nanomechanical Measurement*

Consider the following linear representation of a contact-mechanics model of the tip-sample interaction dynamics,

$$\bar{y}(\ell) = J^*(z_\ell, \theta)\bar{u}(\ell) + \bar{v}(\ell), \tag{8}$$

where $\bar{u}(\ell)$ and $\bar{y}(\ell)$ are the equivalent input and the output in nanomechanical measurements, respectively (see Eq. (3)), $\bar{v}(\ell)$ is the measurement noise of a normal distribution with mean value of $\mu_v$ and variance of $\sigma^2$, i.e., $\bar{v} \sim N(\mu_v, \sigma^2)$, and $J^*(z_\ell, \theta)$ is the discretized linear compliance model. For example, when the truncated Prony series (2) is used, the input-output mapping $J^*(z_\ell, \theta)$ takes the form

$$J^*(z_\ell, \theta) = J_0 - \sum_{i=1}^{n} \frac{J_i(z_\ell - 1)}{(1 + \frac{T}{2\tau_i})z_\ell + (\frac{T}{2\tau_i} - 1)}, \tag{9}$$

where $\theta$ is the vector of unknown parameters (see Eq. (2)), and the measurement frequency $\omega$ is related to the z-transform variable $z_\ell$ through Tustin transformation $j\omega = 2(z_\ell - 1)/T(z_\ell + 1)$.

In the following, the optimal input is obtained through an iterative process: In each iteration, the designed excitation force is applied to the nanomechanical experiment, and the measured force and indentation data are used to estimate the parameters of the compliance model, which, in turn, is utilized to seek the input design for the next iteration. Thus, towards an optimal input, the following linear mapping from the parameters to the estimation-caused error in output is obtained from the first-order Taylor series expansion of the linear compliance model, J(·), around the estimated parameters obtained in the previous iteration, $\theta_k$,

$$\begin{aligned} \Delta\bar{y}(\ell) &\triangleq \bar{y}(\ell) - J^*(z_\ell, \theta_k)\bar{u}(\ell) \\ &= f(\ell)\,(\theta_{k+1} - \theta_k) + \bar{v}(\ell) \triangleq f(\ell)\Delta\theta + \bar{v}(\ell), \end{aligned} \tag{10}$$

where $f(\ell) \in \mathbb{C}^{1\times m}$ $(m = n_a + n_b)$ is given by $\bar{u}(\ell)\,[f_1(\ell), ..., f_m(\ell)]$, with $f_i(\ell) = \partial J^*(z_\ell, \theta_k)/\partial\theta_i$, and $\Delta\theta$ is the difference of the estimated parameters between two successive iterations, i.e., $\Delta\theta = \theta_{k+1} - \theta_k = [\Delta\theta_{k,1}, ..., \Delta\theta_{k,m}]^T$.

Similar to the least-square-based parameter estimation of the ARX model in Sec. II-A, the best linear unbiased estimate (BLUE) of $\Delta\theta$ can be obtained as [7]

$$\begin{aligned} \widehat{\Delta\theta} = &\left[\mathrm{Re}\sum_{\ell=-\frac{N}{2}}^{\frac{N}{2}-1} f^*(\ell)S_{vv}^{-1}(\ell)f(\ell)\right]^{-1} \\ &\left[\mathrm{Re}\sum_{\ell=-\frac{N}{2}}^{\frac{N}{2}-1} f^*(\ell)S_{vv}^{-1}(\ell)\Delta\bar{y}(\ell)\right], \end{aligned} \tag{11}$$

where Re($\mathbb{C}$) denotes the real part of complex number $\mathbb{C}$, and $S_{vv}(\ell) = E[v^*(\ell)v(\ell)]$ is the autocorrelation function of the measurement noise. Thus, by combining Eqs. (8, 10) with the above Eq. (11), an optimal input force can be sought to minimize the covariance of the parameter estimation error, $\mathrm{Cov}\left[\widehat{\Delta\theta}\right]$, which, can be shown [7], [8], is equivalent to the inverse of the Fisher information matrix $M$ [7], i.e.,

$$\min_{\bar{u}(\cdot)} Cov\left[\widehat{\Delta\theta}\right] = \min_{\bar{u}(\cdot)} E[(\widehat{\Delta\theta} - \mu_{\widehat{\Delta\theta}})^2] = \min_{\bar{u}(\cdot)} M^{-1}, \tag{12}$$

where $\mu_{\widehat{\Delta\theta}}$ is the expectation of $\widehat{\Delta\theta}$. Note that for a non-degenerate input design (i.e., an input with the minimum number of different frequencies for the transfer function model with given order [11]), the Fisher information matrix is nonsingular and thereby invertible [11]. Hence the optimal input can be obtained by maximizing the Fisher information matrix, which is equivalent to the minimization of the Cramer-Rao Lower Bound (CRLB), i.e., the lower bound of the variance of the estimation error $\widehat{\Delta\theta}$ [8]. In Eq. (12), the Fisher information matrix, $M$, is given by [12]

$$M = N\ \mathrm{Re}\sum_{n=-N/2}^{N/2-1} E[f^*(n)S_{vv}^{-1}(n)f(n)] \tag{13}$$

From Eq. (13), the Fisher information matrix can be derived as (see [7] for details)

$$M(\omega) = \sum_{\omega=-\pi}^{\pi} \frac{1}{2\pi}\left[\frac{\partial J^*}{\partial\theta_1}, ..., \frac{\partial J^*}{\partial\theta_m}\right]^T S_{vv}^{-1}(\omega)\left[\frac{\partial J}{\partial\theta_1}, ..., \frac{\partial J}{\partial\theta_m}\right]. \tag{14}$$

Next, we consider multi-sinusoidal signals for the maximization of the Fisher information matrix,

$$u(\ell) = \sum_{i=1}^{q} A_i \sin(\omega_i \ell). \tag{15}$$

Such a choice of input is general as for any amplitude-normalized input with a mixed (continuous and discrete) spectrum, an equivalent input with purely discrete spectrum can be found. Moreover, the required number of distinct points in the input frequency spectrum is no more than $[m(m+1)/2+1]$ [7], where $m$ is the number of unknown parameters. Therefore, one can confine the search of the optimal input to the search of optimal frequency components in the sinusoidal input (15).

*Definition 1:* For the multi-sinusoidal input $u(\ell)$ (15), an input design is to determine a finite set $F$ consisting of pairs of the input frequency $\omega_i$ and its associated power spectral density function $p(\omega_i)$,

$$F(\omega, p) = \left\{(\omega_1, p(\omega_1)), \cdots, (\omega_q, p(\omega_q))\right\}, \qquad (16)$$

such that each power spectral density p($\omega_i$) equals to the amplitude $A_i$ of that frequency $\omega_i$ over the mean square power $\sigma_u^2$ of the input $u(t)$, i.e., $p(\omega_i) = A_i/(2\pi\sigma_u^2)$, where $\sigma_u^2$ is the mean square power of $u(t)$, i.e., $\sigma_u^2 = \frac{1}{2\pi}\sum_{i=1}^{q} A_i$.

With the above definition, the optimal input design $F^*$ amounts to the search of the optimal frequency component $\omega_i$ through the iteration process. Specifically, after each iteration $k$, one candidate optimal frequency $\omega_k$ will be obtained that maximizes the following cost function,

$$\max_{\omega} d_k(\omega, F) = \frac{\partial J(z_\ell, \theta_k)}{\partial \theta} M^{-1}(\omega_F) \frac{\partial J^*(z_\ell, \theta_k)}{\partial \theta} \rightarrow \omega_k \quad (17)$$

where '*' denotes the optimal solution when maximizing the cost function , and $M(\omega_F)$ is the Fisher information matrix evaluated at the input frequencies $\omega_i$ selected in each iteration, $M(\omega_F) = \sum_{i=1}^{q} M(\omega_i)$, where $\omega_i$s are the input frequencies in the current input design $F(\omega, p)$.

Comparison of the above cost function (17) with Eq. (14) implies that the maximization of the cost function $d(\omega, F)$ is equivalent to the maximization of the Fisher information matrix $M(\omega)$ [11]. Various criteria have been proposed to maximize the Fisher information matrix. In the proposed optimal input design approach, D-optimal criterion is chosen for the D-optimality is invariant to the parameter scale and linear transformations of the output. The D–optimality, in this paper, is obtained through the one dimensional search algorithm, where the new candidate optimal frequency $\omega_k$ is obtained by computing and then comparing the cost function $d_k(\omega, F)$ at every sampling frequency within the measured frequency range.

The corresponding power spectral density function for the optimal candidate frequency $\omega_k$, $p(\omega_k)$, is selected by choosing the corresponding spectral $\alpha_i$ (see Eq. (18)) from a pre-specified sequence $\{\alpha_1, \alpha_2, \cdots\}$ satisfying

$$0 \le \alpha_k \le 1, \ \sum_{k=1}^{\infty} \alpha_k = \infty, \text{ and } \lim_{k\rightarrow\infty} \alpha_k = 0, \qquad (18)$$

and the power spectral density of other frequency components already-existing in the input design $F(\omega)$ are updated by adjusting the corresponding amplitude accordingly by

$$p(\omega_k) = (1 - \alpha_k) p(\omega_k), \quad \text{for } k = 1, 2, \cdots, \text{ and } k \neq j \quad (19)$$

The above iteration process to optimize the input is conducted until the variation of the identified parameters of the compliance model is within the chosen threshold.

### C. Implementation of the Optimal Excitation Force

To implement the above optimal input force design, control input to the vertical-axis piezoactuator of the AFM needs to be obtained so that the applied excitation force (i.e., the cantilever deflection) will accurately track the desired force profile. The control input must be able to account for the instrument dynamics effects. Or, due to the convolution effect of the input with the instrument dynamics, large distortions in the excitation force occur [4]. Iterative learning control (ILC) is ideal to achieve precision tracking of the desired optimal excitation force. In this paper, we utilized the modeling-free inversion-based iterative control (MIIC) [13] to track the desired force profile.

TABLE I

PARAMETER ESTIMATION RESULTS OBTAINED FROM NUMERICAL SIMULATIONS. THE UNITS FOR $J_i$ AND $\tau_i$ ARE $\mu Pa^{-1}$ AND MS.

| Pa. | Act. | Case1 | Er.% | Case2 | Er.% | Case3 | Er.% |
|---|---|---|---|---|---|---|---|
| $J_0$ | 9.11 | 9.11 | 0 | 7.73 | 15.1 | 9.13 | -0.25 |
| $J_1$ | 2.08 | 2.08 | 0 | -1.03 | 150 | 2.10 | -1.14 |
| $J_2$ | 1.53 | 1.53 | 0 | 3.87 | -147 | 1.68 | -10.1 |
| $J_3$ | 1.51 | 1.50 | 0.66 | 2.07 | -37 | 5.51 | 265 |
| $\tau_1$ | 25.28 | 25.2801 | 0.12 | -34.79 | 238 | 26.25 | -3.85 |
| $\tau_2$ | 2.9 | 2.9004 | 0.01 | 3.71 | -28 | 2.71 | 6.7 |
| $\tau_3$ | 0.474 | 0.4767 | -0.57 | -0.05 | 110 | 0.944 | -99.1 |

## III. SIMULATION AND EXPERIMENTAL EXAMPLE: FREQUENCY-DEPENDENT VISCOELASTICITY MEASUREMENTS OF PDMS

The proposed optimal input design approach is illustrated through the nanomechanical property measurement of a PDMS sample using SPM. Both simulation and experiment were conducted to demonstrate the need and the efficacy of the proposed method.

### A. Simulation Study of Input Force Design

The goal of the simulation studies was two folds: (1) To evaluate the parameter estimation of a given linear compliance model in nanomechanical measurements; and (2) to evaluate and demonstrate the need and efficacy of optimal input design in the identification with or without adding noise to the output data. Specifically, a $3^{rd}$ order Prony series model, J(t), of a PDMS sample was used as the target system to be identified. The parameters of the model, as listed in the second column of Table I, were chosen as those obtained recently in [5]. Since there were 7 unknown parameters in this model, a multi-sinusoidal signal with four frequency components was used as the effective input force (Unit: nano Newton), i.e., $u(\ell) = A\sum_{i=1}^{4} \alpha_i \sin(2\pi f_i \ell)$, where the amplitude of each frequency component was chosen to be the same at A.

Three different scenarios were considered in the simulation. Case 1: The input design based on the a priori knowledge of PDMS viscoelasticity [5] was used in the identification, and no noise was augmented to the effective output of the "true" compliance model when the output was used in the identification; Case 2: the input design was the same as in Case 1) but a band-limited white noise was added to the output (i.e., to mimic the measurement noise effect); and Case 3: the optimal input design by the proposed approach was used and the output noise as in Case 2) was added. In the first case, the frequencies in the input design $F_0 = \{(1, 0.25), (10, 0.25), (100, 0.25), (1000, 0.25)\}$ was chosen based on the knowledge of the complex compliance of polymers. For Cases 2) and 3), a band-limited white noise with signal to noise ratio of 134.3 and 146.7 (with respect to the desired force profile), respectively, was added to the output. In Case 3), the initial choice to search the optimal input

TABLE II

THE FREQUENCY COMPONENTS OF THE OPTIMAL INPUT DESIGN OBTAINED IN THE SIMULATION STUDY

| Fre. (Hz) | 1 | 10 | 30 | 60 | 83 | 92 | 79 | 93 |
|---|---|---|---|---|---|---|---|---|
| Amp. (%) | 25 | 25 | 10.7 | 10.7 | 7.15 | 7.15 | 7.15 | 7.15 |

design was set as that used in Case 1) originally, and then changed to $F_0 = \{(1,0.25),(10,0.25),(30,0.25),(60,0.25)\}$ for faster convergence when there existed output noise. The frequency range to search was thereby limited to [1, 100] Hz, and the coefficient $\{\alpha_k\}$ for updating the input design was chosen to be $1/(k+3)$ (where k is the number of iteration). The sampling frequency was chosen as 8 KHz.

The output of the $3^{rd}$-order compliance model to be identified was used along with the input to identify the parameters of the discretized linear compliance mapping by using the ARX least-square method (Eq. (7), see Sec. II-A). The parameters of the Prony series model were then obtained from Eq. (5) after discrete-to-continuous conversion. The estimated parameters in the above three cases are listed in Table I, and the obtained optimal input design is specified in Table II. The estimation error of the parameters along the iteration process in Case 3) (i.e., the proposed optimal input design) is also shown in Fig. 2.

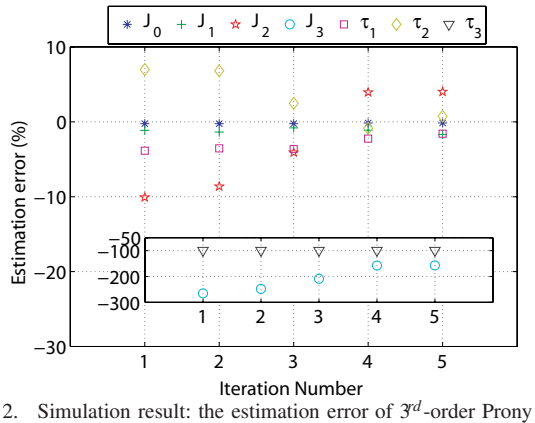


Fig. 2. Simulation result: the estimation error of $3^{rd}$-order Prony series by using the proposed optimal input design in the presence of output noise.

The simulation results demonstrate that optimal input design is needed in nanomechanical measurements. As shown in Table I, when there was no measurement noise, the parameters of the $3^{rd}$-order Prony series model can be accurately estimated by using the input design based on the priori-knowledge of the material—Case 1. Such a high accurate estimation, however, was lost when noise was augmented to the output. As noise is inevitable in real experiment, the simulation results showed that the input force must be carefully designed in nanomechanical measurements.

The simulation results also demonstrated that the proposed optimal input design approach was promising for nanomechanical measurements. By using the proposed optimal input design (Case 3), the estimated parameters converged in five iterations (see Fig. 2). Particularly, the estimation errors of all parameters except the two related to the fastest time constant ($J_3$ and $\tau_3$, see Table I) were small. We note that although the estimation error of the fast part of the compliance model was relatively large, the estimated value was still within the same decade as the true value. Thus, the simulation results served references for the experiments well.

TABLE III

PARAMETER ESTIMATION RESULT WITH OPTIMAL INPUT DESIGN

| Param. | Ite.1 | Ite.2 | Ite.3 | Ite.13 | Ite.14 | Ite.15 |
|---|---|---|---|---|---|---|
| $J_0$ (n$Pa^{-1}$) | 261 | 252 | 250 | 252 | 262 | 251 |
| $J_1$ (n$Pa^{-1}$) | -18 | 4 | -33 | 24 | 20 | 9 |
| $J_2$ (n$Pa^{-1}$) | 121 | 467 | 51 | 83 | 68 | 90 |
| $J_3$ (n$Pa^{-1}$) | 517 | 185 | 1800 | 725 | 608 | 310 |
| $\tau_1$ (ms) | 212.3 | 171.5 | 63.9 | 54.4 | 81.2 | 71.0 |
| $\tau_2$ (ms) | 1.85 | 0.97 | 5.93 | 1.33 | 1.30 | 3.32 |
| $\tau_3$ (ms) | 0.12 | 0.093 | 0.16 | 0.069 | 0.11 | 0.11 |

### B. Experimental Implementation and Discussion

The simulation results were utilized to guide the implementation of the proposed approach to the nanomechanical measurement on a PDMS sample in experiments. Based on the simulation, the initial choice of the input design used in Case 3) of the simulation was used as the initial input design in the experiments. The sampling frequency was further reduced to 2 kHz in the experiments to reduce the measurement noise effect. An analog filter was also added to further attenuate the output noise. The desired cantilever deflection was tracked accurately by using the recently developed MIIC technique (the 2-norm and infinity-norm tracking error was below 2% and 5%, respectively).

During each iteration of the search for the optimal input design, the indentation in the PDMS (produced by the excitation force applied) was needed to identify the parameters of the $3^{rd}$-order Prony series model. The indentation was obtained from the difference of the deflection measured on the PDMS sample and that on a hard reference sample (e.g., a sapphire sample in this experiment) when the same control input (to drive the piezoactuator) was applied in both force-curve measurements. To avoid the switching back and forth between the hard and the soft (PDMS) samples during the iterations of the optimal input design process, thereby reduce the measurement errors, the deflection on the hard reference sample was estimated by applying the same control input (obtained by using the MIIC technique) to the model that captures the dynamics from the piezo actuator to the cantilever deflection on the hard sample.

The force applied from the tip to the sample during the force measurements can be obtained from the measured cantilever deflection signal as [1], $F_S = K_t \times C_t \times d_S$, where $K_t$ is the stiffness constant of the cantilever, $C_t$ is the sensitivity constant of the deflection signal vs. the vertical displacement of the tip (both can be experimentally calibrated [14]), and $d_S$ denotes the cantilever deflection on the soft sample. The cantilever stiffness $K_t = 0.065$ N/m and the deflection-to-displacement sensitivity $C_t = 85$ nm/V were calibrated experimentally. Then, the indentation of the tip into the PDMS sample was obtained as $Z_I = C_t \times (d_H - d_S)$, where $d_H$ and $d_S$ denote the deflection on the sapphire sample and that on the PDMS sample, respectively, when the same control input was applied in both force-curve measurements.

In the experiments, specifically, two different scenarios were considered: (1) experimental results without optimal input design, and (2) experimental results with optimal input

TABLE IV

THE OBTAINED OPTIMAL FREQUENCIES BY THE EXPERIMENT ON PDMS

| Fre. (Hz) | 1 | 10 | 30 | 60 | 56 | 61 | 67 | 71 | 73 | 84 | 87 | 89 | 95 | 97 | 98 | 99 |
|---|---|---|---|---|---|---|---|---|---|---|---|---|---|---|---|---|
| Amp.(%) | 25 | 25 | 5.54 | 5.54 | 2.78 | 2.78 | 2.78 | 2.78 | 2.78 | 2.78 | 5.56 | 2.78 | 2.78 | 2.78 | 5.56 | 2.78 |

design. In the first case, without optimal input design, the parameter estimation result of the Prony series model was shown in the second column of Table III. In the second scenario, after using optimal input design, the parameter estimation results of the first and last three iterations are shown in Table III and Fig. 3. The obtained optimal frequencies are shown in Table IV.

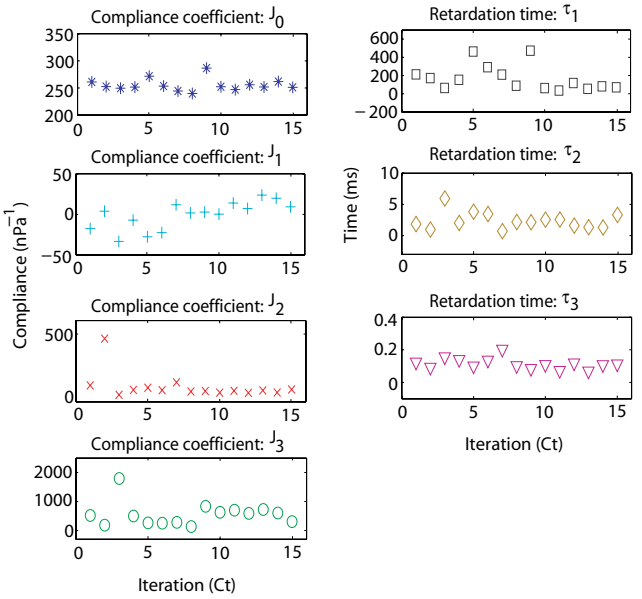


Fig. 3. Experimental parameter estimation result with optimal input design

The experiments demonstrated the efficacy of optimal input design in nanomechanical measurement. For the experiment without optimal input design, as in the second column of Table III, the three time constants were not evenly spaced in each decade. Since the frequencies of input were randomly chosen and the amplitude at each frequency was chosen to be the same, the input design may not be the optimal, and thus we need optimal input design. The Table III shows the experimental results after using optimal input design. Total 15 iterations were conducted. This table shows the first and last three iterations. The estimation results of the time constants were not evenly spaced in the first iteration. As can be seen, the time constants converged and were evenly spaced finally. The Fig. 3 shows the convergence of parameter estimation results after using optimal input design. According to estimated compliance coefficients, the instantaneous modulus of PDMS is about 3.98 MPa and it quickly relaxes to 1.52 MPa. Magnitudes of instantaneous and fully relaxed modulus compare well with DMA tests on the same samples. At room temperature, PDMS is above its glass temperature and displays a clear viscoelastic solid response. Our proposed control-integrated optimal input design and parameter estimation approach clearly captures the rate dependent viscoelastic nature of the PDMS polymer. Therefore, experimental results demonstrate the efficacy of our method for rapid broadband viscoelastic characterization.

## IV. CONCLUSION

In this paper, a new control-integrated optimal input design approach was proposed. In the proposed approach, inversion-based iterative learning control is used to precisely apply the excitation force on sample. Optimal input design is used to search for the optimal input to compensate for the adverse effect of the instrument dynamics, the measurement noise and disturbance. Numerical simulations are conducted to verify the parameter estimation and optimal input design. The proposed approach was also illustrated by implementing it to identify the linear compliance model of a PDMS sample. The proposed approach can be used to characterize the rate dependent viscoelastic nature of soft materials at high speed and broad frequency range.

## REFERENCES


[1] H.-J. Butt, B. Cappella, and M. Kappl, "Force measurements with the atomic force microscope: Technique, interpretation and applications," *Surface Science Reports*, vol. 59, pp. 1–152, 2005.

[2] A. S. A. Syed, K. J. Wahl, R. J. Colton, and O. L. Warren, "Quantitative imaging of nanoscale mechanical properties using hybrid nanoindentation and force modulation," *Journal of Applied Physics*, vol. 90, no. 3, pp. 1192–1200, 2001.

[3] J. R. Lozano and R. Garcia, "Theory of multifrequency atomic force microscopy," *Physical Review Letters*, vol. 100, pp. 1–4, Feb. 2008.

[4] Z. Xu and Q. Zou, "A model-based approach to compensate for the dynamics convolution effect on nanomechanical property measurement," *Journal of Applied Physics*, vol. 107, no. 5, 2010.

[5] Z. Xu, K. Kim, Q. Zou, and P. Shrotriya, "Broadband measurement of rate-dependent viscoelasticity at nanoscale using scanning probe microscope: Poly(dimethylsiloxane) example," *Applied Physics Letter*, vol. 93, pp. 133103–133105, 2008.

[6] H. F. Brinson and L. C. Brinson, *Polymer Engineering Science and Viscoelasticity: An Introduction*. Springer, 2007.

[7] R. K. Mehra, "Frequency-domain synthesis of optimal inputs for linear system parameter estimation," *Journal of Dynamic Systems, Measurement, and Control*, vol. 98, no. 2, pp. 130–138, 1976.

[8] S. M. Kay, *Fundamentals of Statistical Signal Processing, Volume 1: Estimation Theory*. Prentice Hall, 1993.

[9] G. Binnig, C. F. Quate, and C. Gerber, "Atomic force microscope," *Physical Review Letters*, vol. 56, no. 9, pp. 930–934, 1986.

[10] L. Ljung, *System Identification: Theory for the User*, ch. 2, 6. Prentice Hall PTR, 2$^{nd}$ ed., 1999.

[11] R. K. Mehra, "Optimal input signals for parameter estimation in dynamic systems—survey and new results," *IEEE Transactions on Automatic Control*, vol. 19, no. 6, pp. 753–768, 1974.

[12] C. R. Rao, *Linear Statistical Inference and its Applications*. Wiley, New York, 1965.

[13] K.-S. Kim and Q. Zou, "Model-less inversion-based iterative control for output tracking: Piezo actuator example," in *Proceedings of American Control Conference*, (Seattle, WA), pp. 2710–2715, June 2008.

[14] J. L. Hutter and B. J., "Calibration of atomic-force miscroscope tips," *Review of Scientific Instruments*, vol. 64, no. 7, pp. 1868–1873, 1993.